

# Massive black holes in dwarf spheroidal galaxy haloes?

Shoko Jin<sup>1,2\*</sup>, Jeremiah P. Ostriker<sup>1</sup> & Mark I. Wilkinson<sup>1</sup>

<sup>1</sup>*Institute of Astronomy, University of Cambridge, Madingley Road, Cambridge, CB3 0HA, U. K.*

<sup>2</sup>*Clare College, University of Cambridge, Trinity Lane, Cambridge, CB2 1TL, U. K.*

Accepted for publication in MNRAS

## ABSTRACT

It is now established that several of the Local Group dwarf Spheroidal galaxies (dSphs) have large mass-to-light ratios. We consider the possibility that the dark matter in the haloes of dSphs is composed of massive black holes with masses in the range  $10^5 M_\odot$  to  $10^7 M_\odot$ . We use direct  $N$ -body simulations to determine the long term evolution of a two-component dSph composed of a pressure-supported stellar population within a black hole dominated halo. The black holes are initially distributed according to a Navarro, Frenk & White profile. For black hole masses between  $10^5 M_\odot$  and  $10^6 M_\odot$ , the dark matter halo evolves towards a shallower inner profile in less than a Hubble time. This suggests that black holes in this mass range might provide an explanation for the origin of the dark matter cores inferred from observations of Low Surface Brightness galaxy rotation curves. We compare the simulated evolution of the stellar population with observed data for the Draco dSph and find that dynamical heating generally leads to the rapid dispersal of the stellar population to large radii. The dependence of the heating rate on the black hole mass is determined, and an upper limit of  $10^5 M_\odot$  is placed on the individual black holes comprising the dark matter halo of Draco, if its present stellar distribution is representative of the initial one. We also present a simple scaling argument which demonstrates that the dynamical heating of an initially compact, though not self-gravitating, stellar distribution might produce a remnant distribution similar in extent to Draco after 10 Gyr, even for black hole masses somewhat in excess of  $10^5 M_\odot$ .

**Key words:** dark matter — galaxies: dwarf, haloes — methods:  $N$ -body simulations

## 1 INTRODUCTION

The existence of dark matter in the Universe, which has an abundance six times that of baryonic matter, is inferred from sources as diverse as the disk rotation curves of spiral galaxies, gravitational lensing studies of galaxy clusters, the very high mass-to-light ratios of nearby dwarf galaxies and analysis of Cosmic Microwave Background fluctuations. However, the actual composition of the dark matter in the Universe is as yet unknown (Ostriker & Steinhardt 2003). One method by which dark matter may be detected and its properties probed is by means of substructure lensing (e.g. Metcalf & Madau 2001; Li & Ostriker 2002; Keeton 2003). Dark matter studies in the Local Group can also yield constraints on dark matter models via the mass density as inferred from kinematic measurements (e.g. Wilkinson et al. 2002).

The standard cold dark matter (CDM) cosmology, though popular and well-tested on large scales, has some unresolved issues. The two best known are the over-abundance

of low-mass satellite haloes identified at the present epoch in cosmological simulations relative to the number of observed Local Group satellites (e.g. Moore et al. 1999) and the much-debated inner profile of CDM haloes (e.g. de Blok & Bosma 2002; Swaters et al. 2003). The latter may be due to resolution issues in the simulations, where a range of inner density slopes are found by various authors (see Suto 2002, for a concise summary). Low mass haloes may also have intrinsically softer inner profiles than more massive systems (Ricotti 2003). Observationally, there is considerable evidence that massive galaxies also do not have cusped haloes, but instead contain roughly uniform density cores (e.g. Binney & Evans 2001; Salucci 2001; Borriello et al. 2003). The issue of the missing satellite haloes may be due to the fact that some of the satellite galaxies are very diffuse; a few bound stellar systems may therefore be undetected simply due to their low surface brightness (Mateo 1998). It has also been suggested that the satellite crisis can be resolved if all the Local Group dwarf spheroidal galaxies (dSphs) lie in significantly more massive haloes than those implied by previous estimates, which were based only on their central velocity dispersions (e.g. Stoeckl et al. 2002;

\* e-mail: shoko@ast.cam.ac.uk

Hayashi et al. 2003). However, differences between the radial distribution of massive satellite haloes about their parent galaxies in simulations and the observed distribution of the Milky Way dSphs suggest that this cannot be the complete solution to this problem (e.g. De Lucia et al. 2004). Another possibility is that there may exist dark matter haloes which do not harbour a stellar population.

In order to address these issues, some alternatives to CDM have been proposed: these include warm dark matter and self-interacting dark matter (e.g. Spergel & Steinhardt 2000; Gnedin & Ostriker 2001). An interesting complete alternative to dark matter has also been suggested for the observed dwarf Spheroidals (dSphs) whereby special phase-space characteristics permit the long-lived remnant of a tidally disrupted satellite to assume the appearance of a dSph in projection (Klessen & Kroupa 1998); however, difficulties in reproducing the data on Draco have recently been noted in this model (Klessen et al. 2003).

There has been considerable interest in cosmological CDM simulations in the past decade, with a variety of halo profile fits being presented by different authors. Following a set of large cosmological simulations, Navarro et al. (1996, 1997) proposed a universal density profile to accommodate virialised CDM haloes of all masses, which has become commonly known as the NFW profile. The density in the inner region is cusped as  $r^{-1}$ , whereas at larger radii it is proportional to  $r^{-3}$ , with the location of the transition being defined by a scale radius used to characterise the profile. Several authors have subsequently confirmed the fit provided by the NFW profile, although others have also presented steeper inner slopes for the halo density (e.g. Fukushige & Makino 2001; Ghigna et al. 2000; Colin et al. 2003). A generalised density law has therefore been suggested, for which the original NFW profile is a special case, in order to account for such findings (e.g. Zhao 1996). As long as the dark matter is cold and collisionless, the halo profile would not be expected to depend on the nature of the dark matter and, more specifically, it should be independent of the dark matter particle mass. This remains true unless we consider particles whose masses are much greater than a solar mass, for which two-body dynamical effects would become relevant. Such phenomena would first be observed in the lowest mass, lowest velocity dispersion systems such as the dSphs.

Much interest in recent years has been focused on the study of the Local Group satellites, not least because their relative proximity has led to the increased availability of high quality data (Irwin & Hatzidimitriou 1995; Mateo 1998), which place stricter constraints on the nature of the dark matter that appears to dominate their gravitating mass. These systems have also received much attention on the modelling and simulation front (e.g. Stoehr et al. 2002; Wilkinson et al. 2002). Amongst those with the highest mass-to-light ratios is the Draco dSph galaxy. At a heliocentric distance of approximately 80 kpc, Draco has been studied extensively and a wealth of kinematic data exists; in particular, measurements of stellar velocities out to large radii are now available (Kleyna et al. 2002; Wilkinson et al. 2004). Given that within the region probed by the stellar distribution it also appears to have suffered relatively little from the tidal effects of the Milky Way (Odenkirchen et al. 2001a; Klessen et al. 2003; Wilkinson et al. 2004), unlike

some of the other Local Group satellites such as the Sagittarius dwarf (e.g. Helmi & White 2001), Draco is an ideal candidate with which to study the possible properties of dark matter. Draco is also known to contain an old stellar population with an age of more than 10 Gyr; any model of this galaxy must therefore remain stable for at least this length of time in order to be compatible with this observation.

One conceivable candidate for the dark matter, either as the sole or major component, is an ensemble of massive black holes. These could be primeval, or may have grown by accretion and mergers from a primeval population, or have origins in later non-linear structures. Lacey & Ostriker (1985; hereafter LO85) investigated the way in which a halo of massive black holes would affect the stellar dynamics in the Milky Way and obtained results that are generally consistent with observations. Our present study investigates the dynamical effects of a dark matter halo composed purely of primordial massive black holes on the evolution of the stellar component of a dwarf galaxy. It was shown in LO85 that for a dSph such as Draco, an upper limit for the individual black hole mass would be  $2 \times 10^6 M_\odot$ , based upon stability arguments for both the stellar population and the dark matter halo forming the galaxy. More recently, Mao et al. (2004) have suggested that massive black holes with masses in the range  $10^5 - 10^6 M_\odot$  may offer a viable explanation for the observed image flux ratios in strong gravitational lens systems. We use direct  $N$ -body simulations to trace the evolution of a model dSph whose initial structural parameters are chosen such that they are compatible with present-day observations of Draco. The stellar population is treated as a cluster of tracer particles, whose evolution is dependent on the potential of the dark halo. The distribution of the halo particles is chosen to follow an NFW profile, whilst the stellar population is given an initial distribution which is described by a Plummer law. We assume the dark matter of the halo to consist entirely of massive black holes, formed prior to the formation of the stellar population. Their masses are chosen to cover a range whose maximum value has, for generality, been taken to be larger than the constraints imposed by LO85; in each simulation, all black holes have the same mass.

In Section 2 we discuss the generation of our simulated models. We present the results in Section 3 along with a discussion in Section 4. In Section 5 we discuss alternative initial conditions for the stellar distribution of dSphs and their implications for black hole haloes. Finally we present a summary and our main conclusions in Section 6.

## 2 SIMULATIONS

A summary of the simulations performed is given in Table 1. The simulations were carried out using the NBODY2 code (Aarseth 2001), modified to incorporate tracer particles orbiting within the underlying potential of the dark matter halo to represent the observed stars. The mass of the system was assumed to be derived entirely from the dark matter. The black hole mass was varied in different runs over the range  $10^5 - 10^7 M_\odot$ . We adopt the standardised  $N$ -body units described by Heggie & Mathieu (1986):  $G = 1$ ,  $M_{\text{tot}} = 1$ , where  $M_{\text{tot}}$  is the total self-gravitating

**Table 1.** Model parameters: Column 1 gives the simulation number; columns 2–4 give the total number of black holes, the mass of a single black hole and the total halo mass respectively; column 5 gives the total number of tracers; column 6 gives an estimate of the initial half-mass relaxation time  $t_{\text{rh}}$  given by equation (11); column 7 gives the corresponding relaxation time for the central 5 percent (by mass) of the black hole distribution; columns 8–10 give the halo scale length, density scale and concentration respectively; column 11 gives the length conversion from  $N$ -body units to physical distances in kpc; column 12 gives the gravitational softening  $\epsilon$  (in  $N$ -body units) used.

Model	$N_{\text{BH}}$	$M_{\text{BH}}$ ( $10^6 M_{\odot}$ )	$M_{\text{total}}$ ( $10^9 M_{\odot}$ )	$N_{\text{tr}}$	$t_{\text{rh}}$ (Gyr)	$t_{\text{r0}}$ (Gyr)	$r_s$ (kpc)	$(10^5 \rho_{\text{crit}})$	$c$	$r_{\text{phys}}$ (kpc)	$\epsilon$
1.....	1001	1.0	1.0	–	3.4	0.07	0.6	10.4	32.6	5.5	0.02
2.....	101	10.0	1.0	$10^4$	0.5	0.02	0.6	10.4	32.6	4.3	0.02
3.....	300	3.3	1.0	$10^4$	1.2	0.05	0.6	10.4	32.6	4.9	0.02
4.....	1001	1.0	1.0	$10^4$	3.4	0.07	0.6	10.4	32.6	5.5	0.02
5.....	1001	1.0	1.0	$10^5$	3.4	0.08	0.6	10.4	32.6	5.5	0.0002
6.....	1001	1.0	1.0	$10^5$	3.4	0.08	0.6	10.4	32.6	5.5	0.02
7.....	3001	1.0	3.0	$10^5$	7.3	0.19	1.2	5.2	16.3	7.1	0.02
8.....	3000	0.3	1.0	$10^4$	8.5	0.12	0.6	10.4	32.6	5.1	0.02
9.....	3000	0.3	1.0	$10^5$	8.5	0.12	0.6	10.4	32.6	5.1	0.02
10....	9002	0.3	3.0	$10^5$	19.5	0.45	1.2	5.2	16.3	7.2	0.02
11....	10001	0.1	1.0	$10^4$	24.9	0.49	0.6	10.4	32.6	5.2	0.02

mass, and the initial total energy  $E_0 = -1/4$ . The inclusion of a gravitational softening parameter  $\epsilon$ , or softening length, ensures that force singularities do not occur as the separation of particles tends to zero. A value of  $\epsilon = 0.02$  in  $N$ -body units, chosen for computational expediency, was used for the majority of our simulations, corresponding to a physical length of  $86 \text{ pc} < \epsilon < 144 \text{ pc}$  depending on the model. Model 5 was performed as a repeat of model 6, but with the softening length reduced by a factor of 100, in order to verify that we had not missed any significant physical effects as a result of using relatively large softening in the other models. The number of tracers at the start of the simulation was 10,000 for models 2–4, 8 and 11, and 100,000 for the remaining models. All simulations were performed on the Sun Workstation Cluster at the Institute of Astronomy and allowed to run to at least 20 Gyr.

## 2.1 Initial Conditions

The NFW density profile (Navarro et al. 1996, 1997), proposed as a universal fitting formula for CDM haloes which form in a hierarchical clustering scenario, has the form:

$$\rho(r) = \frac{\rho_s r_s^3}{r(r + r_s)^2}, \quad (1)$$

where the parameters  $\rho_s$  and  $r_s$  used to characterise the NFW profile are the density scale and scale radius respectively.

The black holes in our simulations are initially distributed according to the NFW profile. The allocation of the initial particle velocities is performed by numerically evaluating the velocity dispersion using the Jeans equation for a spherically symmetric system (e.g. Binney & Tremaine 1987),

$$\frac{1}{\nu} \frac{d(\nu \sigma^2)}{dr} = -\frac{d\Phi}{dr}, \quad (2)$$

where  $\nu(r)$  is the halo density profile,  $\sigma(r)$  is the one dimensional velocity dispersion for the halo and the underlying halo potential is  $\Phi(r)$ . We have assumed velocity isotropy

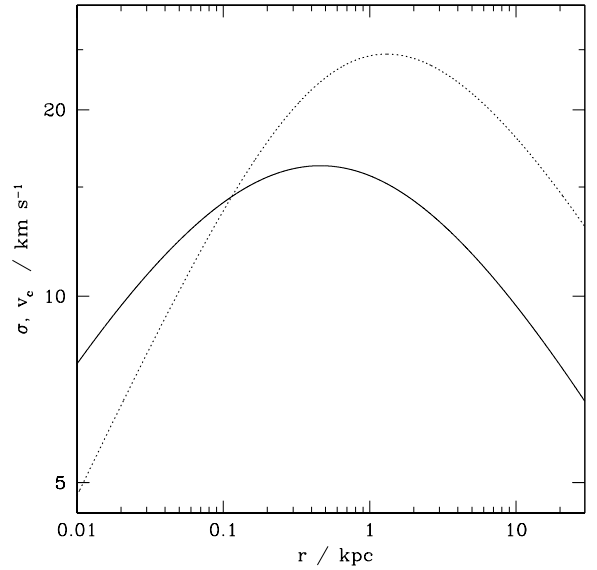


**Figure 1.** The velocity dispersion  $\sigma$  (solid curve) and circular velocity  $v_c$  (dotted curve) of the halo particles as a function of radius. The initial velocities of the massive particles are generated from this distribution for all models except models 7 and 10 in which the halo scale length  $r_s$  is larger.

for the halo particles, which gives a satisfactory fit to the results observed in cosmological simulations. In this case,  $\sigma(r)$  has the form

$$\sigma^2 = 4\pi G \rho_s r_s^2 (s_{\text{max}} - s_x) x (1 + x)^2, \quad (3)$$

where  $x$  is the scaled radius  $r/r_s$  and  $s_x$  is given by

$$s_x = \int_0^x \frac{\ln(1+x') + (1+x')^{-1} - 1}{x'^3(1+x')^2} dx'. \quad (4)$$

The value of  $s_{\max}$  was evaluated by numerically integrating up to a sufficiently large radius. The form of the one dimensional dispersion so derived is shown in Fig. 1, which also shows the circular velocity profile for the NFW halo.

For each particle, we randomly generate a velocity from a Maxwellian velocity distribution with velocity dispersion calculated using equation (3) at the position of the particle. While at each place the total energy (gravitational and kinetic) of the local particles is correct and the Jeans equation is satisfied, we note that recent work by Kazantzidis et al. (2004) has found that the assumption of a Maxwellian velocity distribution can lead to a re-adjustment and short-term spurious evolution in  $N$ -body simulations, due to the fact that the true velocity distribution is not an exact Maxwellian. However, this evolution does not have a significant impact on the simulations we present in this paper. The initial re-adjustment takes place on a short time scale (the halo crossing time) while the effects we are studying take place on the much longer halo relaxation time scale.

We note in passing that it is possible to relate the maxima of the rotation curve  $v_{\max}$  and velocity dispersion  $\sigma_{\max}$  of an NFW halo, and the corresponding radii  $r_1$  and  $r_2$ , to  $\rho_s$  and  $r_s$  via

$$v_{\max}^2 = 2.717G\rho_s r_s^2 \quad \sigma_{\max}^2 = 1.185G\rho_s r_s^2 \quad (5)$$

and

$$r_1 = 2.163r_s \quad r_2 = 0.763r_s. \quad (6)$$

The numerical constants were obtained by direct evaluation of the circular speed and velocity dispersion profiles. As Fig. 1 also shows, the maxima of the two profiles do not occur at the same radius.

We represent the dSph stellar population by tracer particles. This is justified on the basis that several of the dwarf satellites of the Milky Way are observed to have very high mass-to-light ratios; in particular, Draco is known to have an extremely large mass-to-light ratio of 350–1000 in solar units (Kleyna et al. 2001). These systems therefore appear to be very dark matter dominated, with their stellar populations residing in massive dark haloes. In our simulations, the tracers are initially distributed according to a Plummer profile, which is known to provide a good fit to the present light distribution in the inner regions of certain dSphs, including Draco. The form of the three dimensional Plummer (1911) luminosity distribution  $\nu(r)$  is given by

$$\nu(r) = \frac{\nu_0 r_P^5}{(r_P^2 + r^2)^{5/2}}, \quad (7)$$

where the scale length  $r_P$  corresponds to the projected half-light radius of the model. For Draco,  $r_P$  is approximately 232 pc, which implies a core radius (the radius at which the surface brightness falls to half its central value) of 150 pc. The tracer velocities are again obtained by means of the Jeans equation (2). As before, we assume velocity isotropy, as suggested by the observed stellar kinematics of Draco (Kleyna et al. 2002).

The halo parameters for the majority of our simulations are chosen to reflect the observational estimates of the mass of Draco (Kleyna et al. 2001). The halo mass is constrained

by requiring that the value of  $M_{200}$ , the mass contained within a radius  $r_{200}$  which encompasses a mean overdensity of 200 times the critical density, yields a mass within  $3r_P$  which is consistent with that of Draco. The scale length of the halo is given by  $r_s = r_{200}/c$ , where the ‘concentration’  $c$  of the halo is set using the scaling relation of Bullock et al. (2001):

$$c = 9 \left( \frac{M_{200}}{M_*} \right)^{-0.13}, \quad (8)$$

where  $M_* = 2.14 \times 10^{13} M_\odot$  is the typical collapsing mass at the present epoch. The value of  $r_{200}$  is then given by

$$r_{200} = \left( \frac{3M_{200}}{800\pi\rho_{\text{crit}}} \right)^{1/3}, \quad (9)$$

where  $\rho_{\text{crit}} = 3H^2/8\pi G$  is the critical density for closure of the Universe; we take  $H = 70 \text{ km s}^{-1} \text{ Mpc}^{-1}$ . The relation between the concentration and the other parameters is made complete by the alternative description of the density scale as  $\rho_s = \delta_c \rho_{\text{crit}}$  where

$$\delta_c = \frac{200}{3} \frac{c^3}{[\ln(1+c) - c/(1+c)]}. \quad (10)$$

The specification of the halo mass  $M_{200}$  thus allows all other parameters to be deduced using the above relations. While most of our simulated haloes have similar masses to that of Draco, we also include a number of haloes with larger scale radii. This extends our modelling to include Low Surface Brightness (LSB) galaxies.

## 2.2 Relaxation Time Scale

We expect the time scale on which the halo profile evolves to be related to  $t_{\text{rh}}$ , the relaxation time at the half-mass radius of the initial black hole distribution. The relaxation time scale is essentially the time scale over which particles lose memory of their initial energies due to mutual encounters. The half-mass relaxation time for each model, listed in Table 1, is estimated using the definition of  $t_{\text{rh}}$  as given by Binney & Tremaine (1987, chapter 8):

$$t_{\text{rh}} = \frac{2.1 \times 10^9 \text{ yr}}{\ln(0.4N)} \left( \frac{10^6 M_\odot}{m} \right) \left( \frac{M}{10^9 M_\odot} \right)^{\frac{1}{2}} \left( \frac{r_h}{1 \text{ kpc}} \right)^{\frac{3}{2}}, \quad (11)$$

where  $M$  and  $N$  are the total mass and number of black holes in the system respectively,  $m$  is the mass of an individual black hole and  $r_h$  is the half-mass radius. We note that the derivation of equation (11) assumes a Plummer model and is not precisely valid for an NFW profile for which the ratio of the half-mass radius to the gravitational radius is about 15 percent larger than in the Plummer case. Thus, this corresponds to a deviation in  $t_{\text{rh}}$  of less than 5% for our models. However, equation (11) provides a good indication of the typical relaxation time and we have chosen therefore to keep it in its more familiar form.

The dependence of relaxation time on black hole mass demonstrates the conservative nature of our choice of initial parameters for the simulated haloes. Given that massive black holes are, by definition, manifestations of Cold Dark Matter, one might expect their generic density distribution to be similar to an NFW profile. However, this is

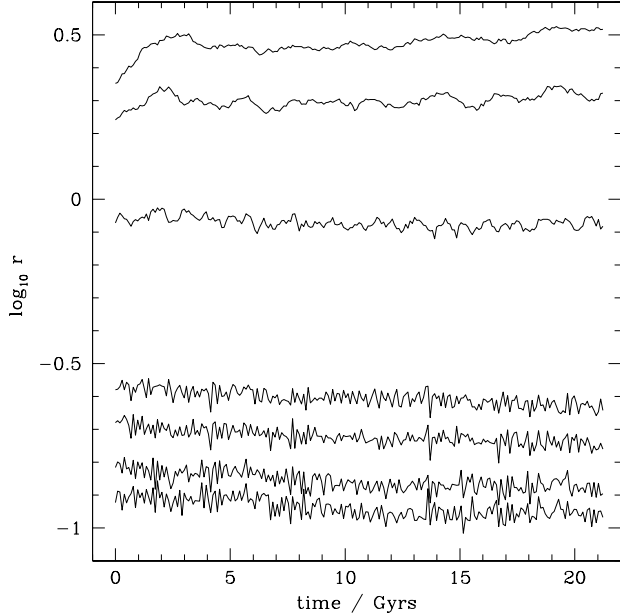


**Figure 2.** The structural evolution of the halo in model 1 as depicted by the Lagrange radii in  $N$ -body units. From the lowest curve upwards, the radii shown correspond to the following halo mass percentiles: 7.5, 10, 15, 20, 50, 75 and 85 percent. The cluster is seen to retain its initial structure over the course of the simulation.

not necessarily the case. For example, if the dark matter consists entirely of  $10^5 M_\odot$  black holes, then a primordial halo of total mass  $10^7 M_\odot$  contains only 100 particles. As we will demonstrate in the next section, a black hole halo with an NFW density profile develops a central core via two-body processes on a time scale of  $t_{\text{rh}}$ . Ostriker & Gnedin (1996) estimate that  $10^7 M_\odot$  haloes become non-linear at a redshift of about  $z = 13$  (see their Figure 1), at which time their virial radius can be shown to be about 0.3 kpc. According to equation (11), the relaxation time for such a halo  $t_{r,7}$  is then about 100 Myr. If this time scale is much less than the difference between the times at which haloes of  $10^7 M_\odot$  and  $10^9 M_\odot$  become non-linear, then we would expect  $10^9 M_\odot$  haloes to be formed from cored sub-haloes. In this case the resulting  $10^9 M_\odot$  haloes would have density profiles which are significantly less cusped than NFW, which would agree with observations of LSB galaxies. In fact, the  $10^9 M_\odot$  haloes become non-linear approximately  $t_{r,7}$  later than  $10^7 M_\odot$  haloes and so it is less clear what the form of the resulting density profile should be. However, the most unfavourable starting point is the NFW profile and our simulations therefore constitute the strictest test of the ability of black hole dark matter to produce cored galaxy haloes.

**Table 2.** Halo parameters at  $T = 0$  and  $T = 15$  Gyr: Column 1 gives the simulation number; column 2 gives the logarithmic slope of the inner halo at  $T = 0$  for those models in which there are sufficient numbers of black holes to give a statistically meaningful estimate; column 3 gives the radius  $r_{\text{max}}$  at which the initial circular velocity profile achieves its maximum value; column 4 gives the maximum value of the initial circular velocity  $v_{c,\text{max}}$ ; columns 5–7: as for columns 2–4 but for the haloes at  $T = 15$  Gyr.

Model	$\alpha$	$T = 0$		$\alpha$	$T = 15$	
		$r_{\text{max}}$ (kpc)	$v_{c,\text{max}}$ ( $\text{km s}^{-1}$ )		$r_{\text{max}}$ (kpc)	$v_{c,\text{max}}$ ( $\text{km s}^{-1}$ )
1.....	-	1.5	24.3	-	1.5	24.2
2.....	-	1.3	25.5	-	0.1	48.4
3.....	-	1.7	25.1	-	0.8	27.6
4.....	-	1.6	24.3	-	1.7	24.6
5.....	-	1.6	24.2	-	1.0	26.7
6.....	-	1.6	24.2	-	1.7	25.3
7.....	-	2.4	30.2	-	2.4	35.5
8.....	1.33	1.3	25.1	0.22	1.3	26.0
9.....	1.15	1.2	25.1	0.00	1.2	25.9
10....	0.15	2.6	34.7	0.00	2.3	35.9
11....	1.12	1.2	24.6	0.33	1.3	25.6

### 3 RESULTS

#### 3.1 Halo Evolution

The stability of a cluster of massive black holes with an NFW profile (and no tracers) was initially assessed in order to determine the validity of our assumption that such a cluster could act as a halo enveloping a stellar population (model 1). As expected from the estimate of  $t_{\text{rh}}$  in Table 1, we find that the cluster retains its initial structure over the duration of the simulation (Fig. 2). The inner regions are not reproduced in this plot: their evolution will be discussed in detail below.

The evolution of the circular velocity profiles for models 2–4, 7, 10 and 11 is shown in Fig. 3. Table 2 summarises the properties of these curves. As will be discussed in Section 4.1, the initial evolution leads to the destruction of the NFW cusp and the formation of a shallower core. This is followed by slow evolution towards core collapse – the time scale for this evolution varies according to the mass of the black holes. The inner slope of the velocity profile becomes steeper for models 7, 10 and 11, indicating a transition from the initial cusp of the NFW profile to a more uniform density core in the central region of the halo. The evolution of the mass within 500 pc of the halo centre as a function of the initial half-mass relaxation time is shown in Fig. 4 for models 2–4 and 11. Models 2 and 3 display a steady increase in the mean density within 500 pc while in model 4, which has better time resolution (at early times) due to its longer  $t_{\text{rh}}$ , the density first decreases on a time scale of  $t_{\text{rh}}$ . This initial decrease in the mass within 500 pc is followed by a slow increase as the system evolves towards core collapse. In model 11, for which 20 Gyr corresponds to less than one relaxation time, the central density is still decreasing at the end of the simulation. Hayashi et al. (2003) observe similar evolution in their simulations of CDM haloes. They find that this variation of the central density profile occurs on the local escape time scale which is approximately 136 times the local (i.e.

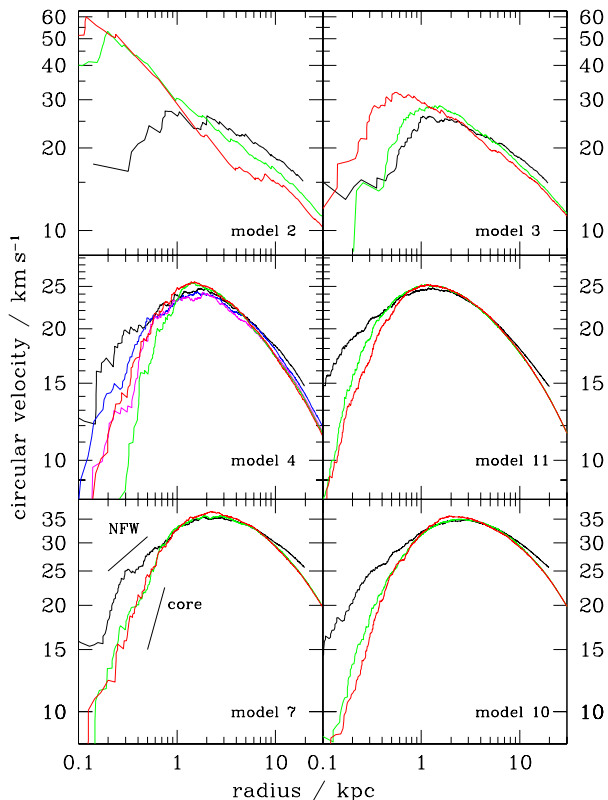


**Figure 3.** Halo rotation curves for models 2–4, 7, 10 and 11 shown at times  $T = 0$  (black), 10 (green) and 20 (red) Gyr. The plot for model 4 also shows the circular velocities at 1 (blue) and 2 (magenta) Gyr. In the panel for model 7, the labelled lines indicate the expected slope for an NFW and a cored density profile.

central) relaxation time scale. As we will discuss later, we find that the evolution proceeds with a characteristic time scale comparable to  $t_{\text{rh}}$ , which is similar in magnitude to the evolutionary time scale observed by Hayashi et al. (2003).

Fig. 3 shows that, after 20 Gyr, the evolution towards core collapse is well advanced only for models 2 and 3. At the opposite end of the mass scale, model 11 has only just developed a core by about 10 Gyr. For model 4, we note that although the inner profile begins to steepen again after 10 Gyr of evolution, the circular speed curve after 20 Gyr indicates that the inner regions remain less cusped than the initial conditions. We conclude that core collapse in black hole haloes will not occur within a Hubble time unless the black hole mass is greater than  $10^{6.5} M_{\odot}$ . Most of the models with black hole masses below this value have the attractive feature that the slope of the cusp *decreases* with time, with the final approximate inner slope being shown in Table 2 for those models for which a statistically meaningful estimate can be made. Thus, NFW haloes composed of black holes with masses in the range  $10^5 M_{\odot}$  to  $10^{6.5} M_{\odot}$  can develop central cores in less than a Hubble time. This may provide an explanation for the origin of the apparent cores in the density profiles of LSB galaxies.

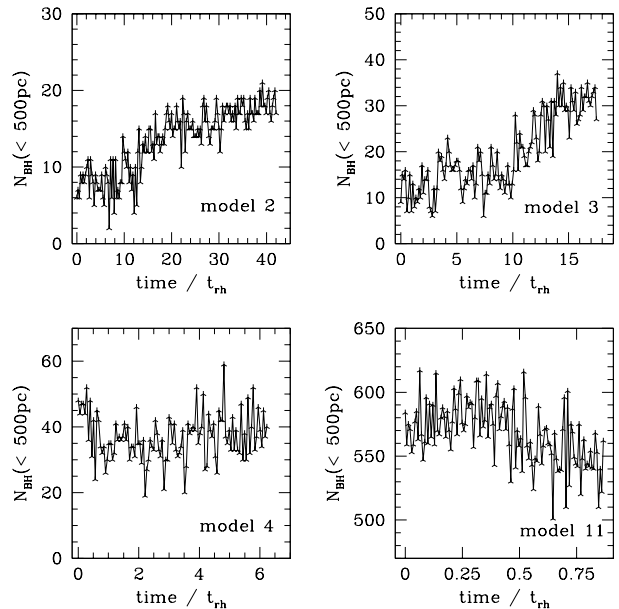


**Figure 4.** The evolution of the number of black holes within 500 pc of the halo centre for models 2, 3, 4 and 11. The time axes of the plots have been scaled individually according to the half-mass relaxation time for each model.

### 3.2 Evolution of the Stellar Population

The evolution of the tracer density profile for some of our models is shown in Fig. 5 where we have assumed each star to have a physical mass of  $1 M_{\odot}$ . In evaluating the projected densities, we have taken radial bins containing 100 tracer particles in each of the three projected (Cartesian) planes. An average value was then calculated for each bin over all three planes. We adopt a similar approach in evaluating the line-of-sight velocity dispersions shown in Fig. 6. The tracer profile becomes extended over the course of the simulation as the particles acquire energy – the heating process is apparent from Fig. 6 where the dispersion is clearly greater for later times. From the evolution of the density in projection, it is straightforward to derive the behaviour of the core radius as a function of time; this is shown in Fig. 7 for models 4 and 6–10. As Fig. 7 shows, in all cases the core radius rapidly increases to values which are inconsistent with the observed value of 150 pc for Draco. Complementary to this is Fig. 8 which shows the decline of the normalized tracer count within 500 pc as a function of time for several models. Unsurprisingly, reduced softening is seen to increase the rate at which the stars are heated; the same effect is seen if we increase the black hole mass. For models utilising  $10^6 M_{\odot}$  black holes, an increase in the halo scale length reduces the rate of heating, whereas for smaller mass black holes, the effect is negligible. As expected, simply increasing the size of the stellar population by a factor of 10 produces no effect as regards the tracer evolution, except that we obtain a better statistical description of the profile. In Section 4.4 we will discuss how a comparison of the core radii of the simulated

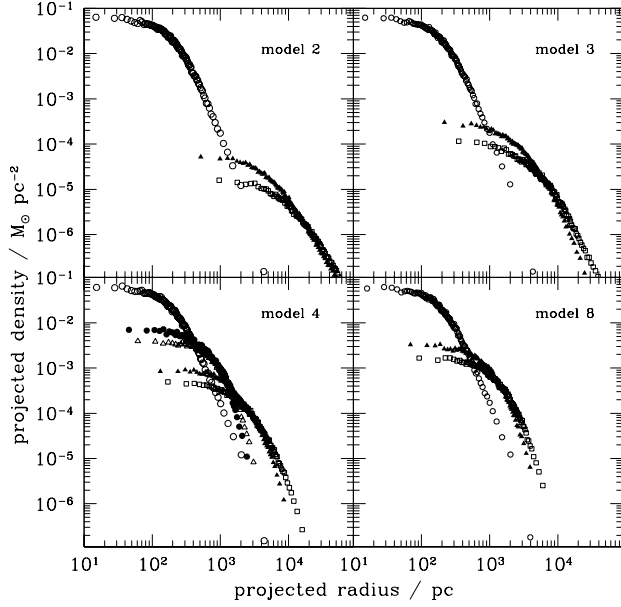


**Figure 5.** Projected tracer density plots for models 2, 3, 4 and 8 shown at times  $T = 0$  (open circles), 10 (filled triangles) and 20 (open squares) Gyr. The plot for model 4 also shows the densities at sampling times of 1 and 2 Gyr with filled circles and open triangles respectively.

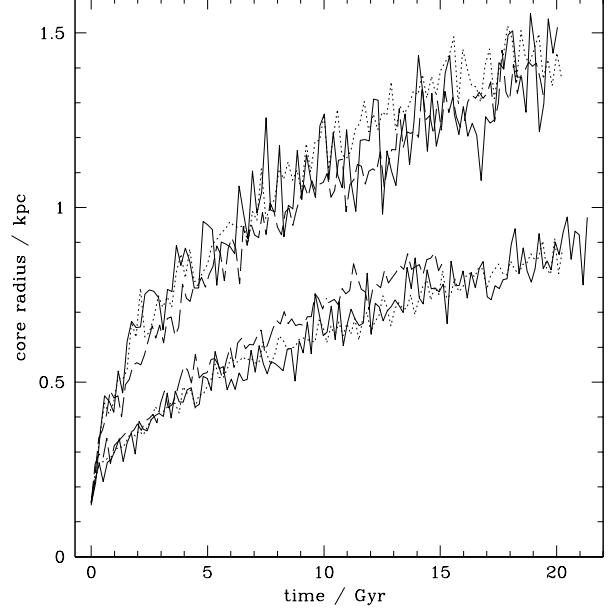


**Figure 7.** The tracer core radius shown as function of time. The upper curves show models 4 (solid), 6 (dotted) and 7 (dashed); the lower curves refer to models 8 (solid), 9 (dotted) and 10 (dashed). Note that the observed core radius of Draco is  $\sim 150$  pc.

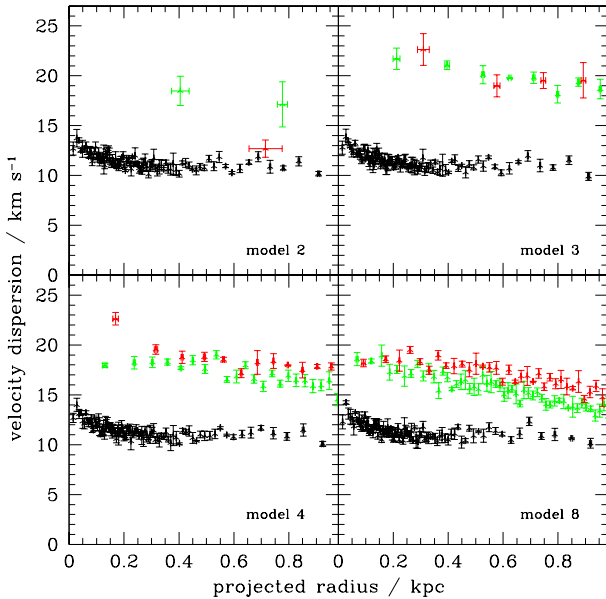


**Figure 6.** Line-of-sight velocity dispersion plots for models 2, 3, 4 and 8 shown at times  $T = 0$  (black), 10 (green) and 20 (red) Gyr.

tracer populations with that of Draco can be used to place a constraint on the mass of individual black holes in the halo of Draco.

The majority of our simulated systems produced no tracer–black hole binaries, although we observe steady black hole–black hole binary formation at all times for all of our models. Tracer–black hole binaries were, however, observed in models 6, 7, 9 and 10, where the first two models produced two binaries each during the course of the simulation, whilst in the latter two models, six and thirteen tracer–black hole binaries were observed respectively. Of these, both models showed one long-lived binary each, corresponding to a bound system lasting up to 340 and 330 Myr respectively. Binaries composed of two black holes were observed frequently and consistently in all simulations, with typically 2–4 transient binaries per sampling time, which corresponds to a stable bound system lasting for approximately 170 Myr (depending on the model); occasionally a binary remained intact for several Gyr. Simply reducing the softening (but not down to zero) did not appear to increase the likelihood of tracer–black hole binary formation, as exemplified by model 5 which showed no tracer bound to a black hole at any time during the course of the simulation. This may be due to two counteracting effects; a reduced softening will allow for closer encounters, but at the same time will increase the heating of the tracer population. This reduces the central density of tracers more rapidly than for a system with a larger softening and decreases the probability of the close encounters which result in the formation of a bound system.

Given that our simulations were performed using non-

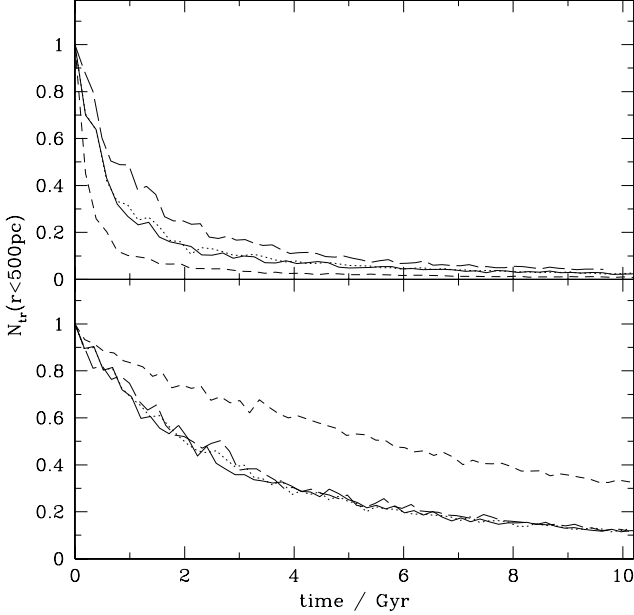


**Figure 8.** Plots showing the decline in tracer number within 500 pc. Top panel: model 4 (solid), model 5 (short dashed), model 6 (dotted), model 7 (long dashed). Bottom panel: model 8 (solid), model 9 (dotted), model 10 (long dashed) and model 11 (short dashed). All models shown in the top panel have black holes of mass  $10^6 M_\odot$ ; those depicted in the bottom panel have black holes of mass  $10^{5.0-5.5} M_\odot$ . Model 4 has  $10^4$  tracers and black holes of mass  $10^6 M_\odot$ ; model 6 is a repeat of model 4 with  $10^5$  tracers; model 5 is a repeat of model 6 with the softening reduced by a factor of 100; model 7 is a repeat of model 6 where the halo scale length has been doubled. Model 8 has  $10^4$  tracers and black holes of mass  $10^{5.5} M_\odot$ ; model 9 is a repeat of model 8 with  $10^5$  tracers; model 10 is a repeat of model 8 where the halo scale length has been doubled; in model 11 the black holes have mass  $10^5 M_\odot$ .

zero force softening, it follows that the rate of binary formation and the dynamical significance of those binaries that do form cannot be properly determined from these models. In order to address these issues, we have re-simulated models 4 and 11 using the NBODY4 code (Aarseth 1999) on the GRAPE-6 special-purpose computer board (Makino et al. 1997) at the Institute of Astronomy, Cambridge. The results are discussed in Section 4.3 below.

We note that in our simulations using the NBODY2 code we treat the stars as tracer particles within the potential of the black hole cluster, thereby allowing improved efficiency in integration time. It then follows that the black holes do not ‘see’ the stars; they simply feel the potential due to the other black holes that are present in the cluster. The stars are tracers within this dark matter potential and their dynamics are unaffected by the stellar population, hence we do not expect to observe tracer-tracer binaries. Note also that all particles are point masses with no internal structure, and hence the formation of a bound two-body system requires a three-body interaction, with the third particle carrying away the excess momentum.

## 4 DISCUSSION

### 4.1 Halo Evolution

In this section, we use simple dynamical models to explain the evolutionary trends of both the black holes and tracers in our simulations. There is an initial decrease in the number of massive particles within 500 pc, where approximately 75 percent of the tracers reside at the start of the simulations. As Fig. 4 shows, this decline occurs on the relaxation time scale  $t_{\text{rh}}$ , and may be explained by the energy exchange between massive particles within the half-mass radius. The inward flow of heat leads to an expansion of the inner halo and a decrease in the central density. This is a manifestation of the inverted temperature profile of the NFW model (see Fig. 1), as compared with the more usually considered Plummer model. We note that such an inversion is not unique to the NFW model, and other profiles exist which also display such an effect (e.g. Dehnen 2003). The analytic dispersion shows that the massive particles at a radius of approximately  $r_s$  are initially hotter than those in both the inner and outer regions. Following this evolution towards an isothermal velocity distribution, the subsequent increase in the number of massive particles within the same region, due to the well understood negative specific heat of self-gravitating systems, may then be described as a slow evolution towards core collapse, similar to what is found in the Plummer model (Cohn 1980). As was mentioned earlier, this evolution was also noted in the simulations of Hayashi et al. (2003).

### 4.2 Stellar Heating Mechanism

The other main effect observed in our simulations is illustrated in Fig. 8, namely the rapid decline in tracer numbers within 500 pc. As the figure shows, reducing the mass of the black holes comprising the halo decreases the rate at which this heating occurs, indicating that the mechanism for the increase in mean stellar kinetic energy is equipartition with the massive particles.

If a system consists of multiple populations with different particle masses, then encounters will tend to lead to the establishment of equipartition of kinetic energies, with the more massive particles losing energy to the less massive particles over time, assuming that velocity was initially independent of mass. As a consequence, the more massive particles will gradually lose kinetic energy and move towards the system centre, whereas the less massive particles will move to larger orbits. The time scale on which equipartition occurs is related to the half-mass relaxation time. In order to check that the rate of heating of the tracers is consistent with kinetic energy equipartition, we calculate the theoretical rate of energy transfer between the two populations given their mean kinetic energies at a specified time. This is given by (Spitzer 1987, eq. 2-60):

$$\frac{d\bar{E}_t}{dt} = 2 \left( \frac{6}{\pi} \right)^{1/2} \frac{m_t n_b \Gamma}{m_b} \frac{(\bar{E}_b - \bar{E}_t)}{(v_t^2 + v_b^2)^{3/2}}, \quad (12)$$

where  $m$  is the mass of an individual particle,  $n$  is the average number density of the black holes,  $\bar{E}$  is the mean particle kinetic energy given by

$$\bar{E}_i = \frac{1}{2} m_i v_i^2, \quad (13)$$



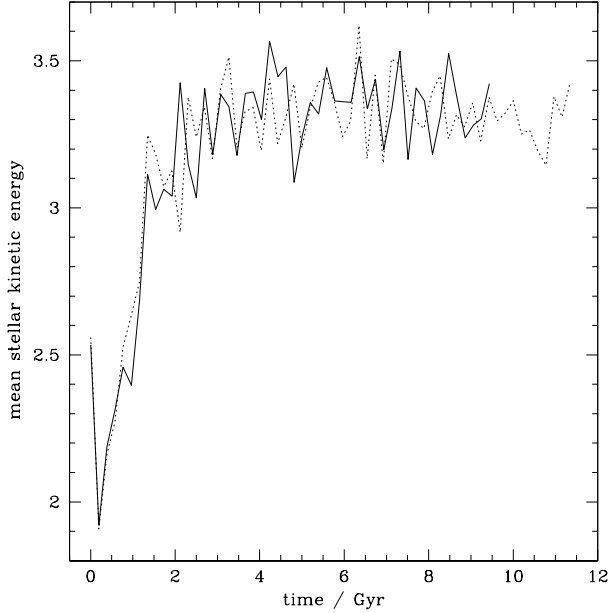


**Figure 9.** The mean tracer kinetic energy (in  $10^{-10}$   $N$ -body units) as a function of time for models 4 (solid) and 6 (dotted). Evolution towards equipartition rapidly results in the tracers acquiring energy from the black holes.

and  $\Gamma$  is defined by

$$\Gamma \equiv 4\pi G^2 m_b^2 \ln \Lambda. \quad (14)$$

The subscripts  $t$  and  $b$  refer to tracer and black hole respectively. Since the halo is observed to evolve on the relaxation time scale at the half-mass radius  $r_h$ , we take  $n$  to be the mean number density within  $r_h$ . The value of  $\Lambda$  in the Coulomb logarithm is given by  $\Lambda = 0.4N$  where  $N$  is the total number of particles of both populations within  $r_h$ .

Equation (12) can be recast in a more transparent fashion by defining  $\bar{\varepsilon}$ , the energy per unit mass of the relevant particle species, and replacing  $n_b m_b$  by  $\rho_b$ . If we consider the limit where  $\bar{E}_b \gg \bar{E}_t$ , then we find

$$\frac{d\bar{\varepsilon}_t}{dt} = 4(6\pi)^{1/2} \frac{v_b^2}{(v_b^2 + v_t^2)^{3/2}} G^2 \rho_b m_b \ln \Lambda. \quad (15)$$

For a fixed mass density in the gravitationally dominant species, the rate of approach to equipartition increases in proportion to the black hole mass and decreases as the cube of the velocity of the tracer particles.

The evolution of tracer energy is shown in Fig. 9 for models 4 and 6, where the rate of energy change is observed to be steady for approximately 2 Gyr. For model 4, the difference in the mean stellar kinetic energy in  $N$ -body units is approximately  $1.12 \times 10^{-10}$  between 0.2 and 2 Gyr which corresponds to 10  $N$ -body time units. The rate of energy transfer according to equation (12) varies as a function of time, but is  $\sim 1.5 \times 10^{-11}$  at 0.2 Gyr and  $\sim 1.1 \times 10^{-11}$  at 2 Gyr. Based on these rates we expect to observe an energy transfer in the range  $(1.1 \sim 1.5) \times 10^{-10}$  units, which agrees well with the energy difference between these two times.

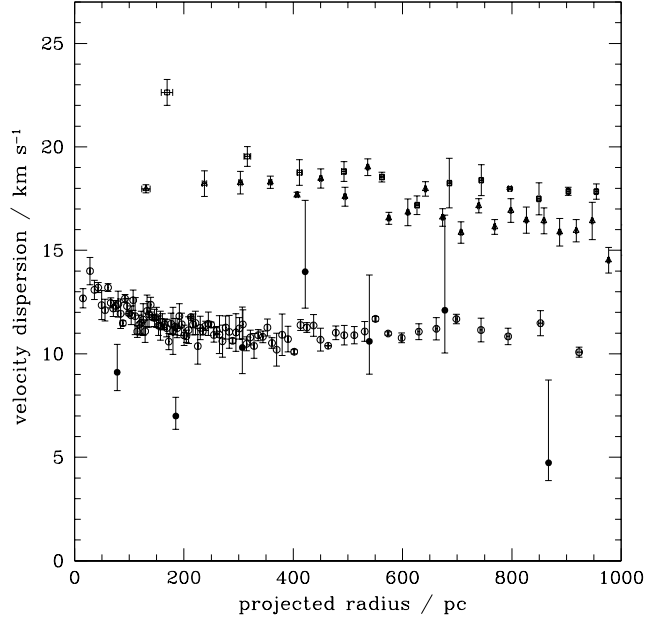


**Figure 10.** One dimensional (line-of-sight) velocity dispersions of model 4 at times  $T = 0, 10$  and  $20$  Gyr (shown with open circles, open triangles and open squares respectively) overplotted with Draco velocity dispersion profile from Wilkinson et al. (2004) (filled circles, with  $1\sigma$  errorbars).

Equation (15) shows that the rate at which the stars gain energy from a population of black holes of mass  $m_b$  and mean spatial density  $\rho_b$  is only weakly dependent on the details of the mass distribution. In order to confirm this, we have performed a number of simulations (not presented in Table 1) in which the halo is represented by a Plummer sphere whose mean density within 3 stellar core radii matches that of the NFW profile in model 4. These simulations confirm that the stellar heating rates for both cored and cusped black hole haloes are almost identical for haloes with similar mean density in the region initially occupied by the stellar distribution.

The formulae given above are based on the assumption that the change in energy of a test particle is due to the cumulative effect of many weak encounters rather than a single close encounter. It is therefore necessary to be aware of the frequency with which tracers experience close encounters with the black holes that may render the use of equation (12) invalid. For models 4 and 6, we find that such encounters are relatively rare, and the results of our energy calculations above confirm that the gradual transfer of energy to the tracers by the black holes initially within  $r_h$  is the main mechanism by which energy is transferred between the two populations. This may be partly due to the value of the softening parameter used in those models which tends to suppress large-angle scattering events.

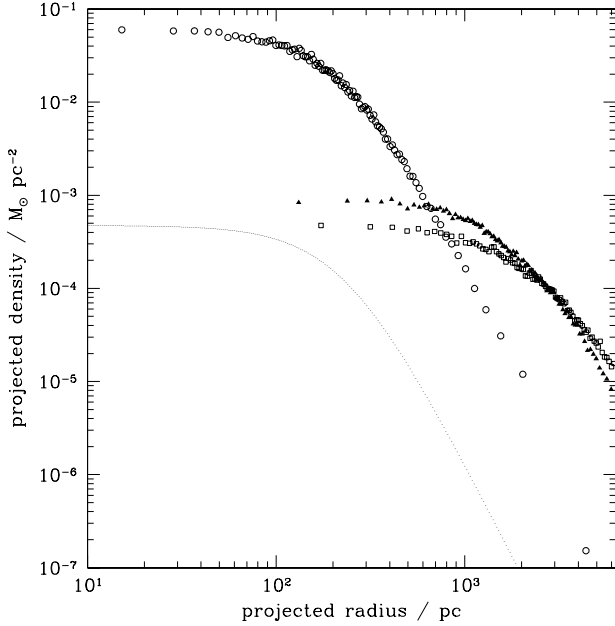


**Figure 11.** Overplot of the tracer density in projection for model 4 and the Plummer profile for Draco. Projected densities at times  $T = 0$  (open circles), 10 (filled triangles) and 20 (open squares) Gyr are shown. The fit to the light distribution of Draco, scaled such that the central density matches the simulated density at 20 Gyr, is given by the dotted line.

#### 4.3 The Effect of Force Softening

Hard black hole-black hole binaries may have an important impact on the dynamics of the entire halo. Softening in turn is a key factor in binary dynamics, from the rate of formation to their rate of destruction. We have re-simulated models 4 and 11 using the NBODY4 code on a GRAPE-6, with the aim of quantifying the effects of a smoothed force-law. Each of the five re-simulations were performed using a different random seed to compute the initial conditions; apart from the exclusion of tracers, all other parameters were kept the same as the original models. Hard binaries (i.e. those with  $|E_{\text{bin}}| > m\sigma^2$  where  $m$  is the mean mass and  $\sigma$  is the velocity dispersion) are identified in these simulations and treated using regularisation, to enable an accurate and efficient treatment of their internal motion (Aarseth 1999; Mikkola & Aarseth 1993, 1998). The results confirmed that the presence of binaries is a very important factor in determining the dynamics of the remainder of the system, with a single binary in the central region being sufficient to cause significant fluctuations in the central density.

In the simulations with  $10^6 M_\odot$  black holes, we observe a relatively steady rate of binary formation and destruction. These binaries tend to form within the inner 1 kpc region and often undergo several companion swaps before being destroyed or expelled. Although this has interesting consequences for the evolution of the inner region of the halo in particular, the fact that we do not observe any binaries in simulations with  $10^5 M_\odot$  black holes, coupled with the dis-

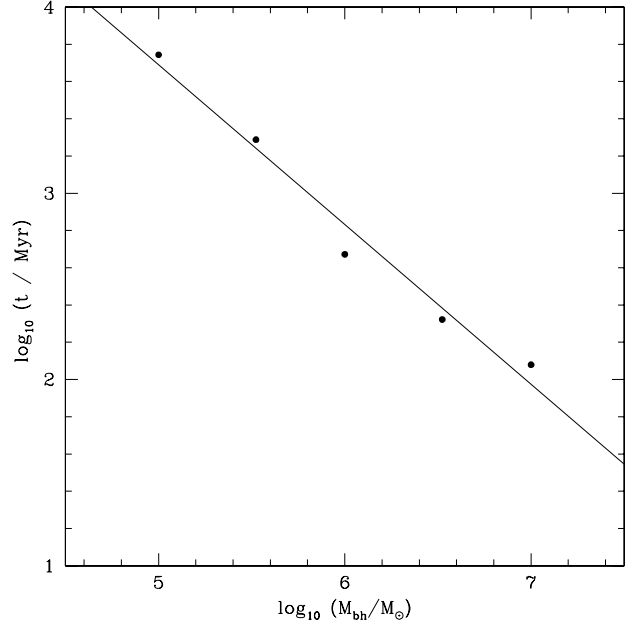


**Figure 12.** Dependence on the individual black hole mass of the time taken for the initial tracer count within 500 pc to drop by a factor of 2. The points show this time for models 2–4, 8 and 11; the curve shows the fit described by equation (16).

cussion below that black hole masses of greater than  $10^5 M_\odot$  are inconsistent with the preservation of the stellar population in Draco, implies that our overall conclusions based on the simulations with softening are unaffected by the inclusion of softening.

#### 4.4 Comparison with the Draco dSph

A comparison of the observed and simulated data can be made by means of the velocity dispersion and projected density shown in Figs. 10 and 11 respectively. The former shows the velocity dispersion profile of Draco overplotted on the dispersions for model 4 at three sampling times, while the latter gives the light distribution at the same times. Also plotted in Fig. 11 is a Plummer profile, which is known to provide a good fit to the light distribution in the inner region of Draco. The profile has been scaled such that the central density matches that of the core density in the simulation at 20 Gyr. The final model density profile in projection is clearly too extended to be compatible with Draco’s observed stellar distribution.

If the halo of Draco is indeed composed of massive black holes, the current extent of the stellar distribution can be used to place an upper limit on the mass of individual black holes, if we assume that there is no spread in the mass of black holes in a halo. In Fig. 12 we plot the time taken for the initial tracer count within 500 pc to drop by a factor of 2 for models 2–4, 8 and 11. We would expect that this time  $t$  would be related to  $t_{\text{rh}}$  for the models and should therefore

scale with mass approximately as  $M^{-0.8}$ , in the mass range we are investigating. In fact, the relation

$$t = \frac{9.549 \times 10^7}{M^{0.858}}, \quad (16)$$

with  $t$  in Myr and  $M$  in  $M_\odot$ , provides a good fit to the results from the simulations as shown in Fig. 12. If we require that the process described above takes at least 5 Gyr, we are able to set an upper limit on  $M$  of  $9.7 \times 10^4 M_\odot$ ; for 10 Gyr, an upper limit of  $4.4 \times 10^4 M_\odot$  would be implied. It should be noted that a drop in the central tracer count by a factor of 2 often corresponds to an increase in the scale radius of the tracer population by a factor of a few and therefore these upper limits are probably overestimates. Thus, black hole masses of less than  $10^5 M_\odot$  are required to prevent significant evolution of the tracer density in a Hubble time; if Draco's initial stellar distribution was similar to that observed today then black hole masses in excess of  $10^5 M_\odot$  can immediately be ruled out.

It is worth noting that black hole masses below  $10^5 M_\odot$  are a priori less interesting as dark matter candidates for a number of reasons. First, as LO85 have shown, black hole masses of approximately  $10^6 M_\odot$  are required to explain the heating of the Milky Way disk. Second, haloes comprising lower mass black holes evolve significantly more slowly than haloes of more massive holes and a halo which formed with a dark matter cusp would, therefore, not develop a core in less than a Hubble time. We therefore conclude that if it could be demonstrated that Draco's stellar distribution has not changed significantly over a Hubble time, then the two primary motivations for adopting black holes as dark matter candidates would disappear.

Another consideration is whether our restricted choice of initial conditions would affect our black hole mass limits. We have made a number of simplifying assumptions in our choice of initial conditions. First we assume spherical symmetry for our halo distributions. This is a reasonable starting point since dSphs such as Draco are observed to have an ellipticity of the stellar distribution of only  $\epsilon_p \simeq 0.3$  (Mateo 1998). The ellipticity of the underlying potential is typically about 1/3 that of the density (e.g. Binney & Tremaine 1987) and the spherical symmetry is probably a good approximation to Draco. Second, we assume that the dSph evolves in isolation – as discussed earlier, observations of Draco suggest that it has been only weakly affected by the tidal field of the Milky Way. Third, we have assumed that all our black holes have the same mass – this effectively means that we are assuming a strongly peaked black hole mass function. The key point with regard to our models is that including any of the above effects e.g. a spectrum of black hole masses or an external tidal field would serve to speed up the evolution of the black hole halo (Giersz & Heggie 1997). Our simulations therefore represent a lower limit to the expected rate of halo evolution. The inclusion of a spectrum of black hole masses could reduce the time to core collapse to  $\sim 1t_r$  (Giersz & Heggie 1996). From Table 1, allowing for the initial evolution of the NFW profiles towards a core, models in which the peak of the black hole mass function is less than about  $10^{5.5} M_\odot$  are still unlikely to reach core collapse within a Hubble time. On the other hand, models with a mass peak around  $10^6 M_\odot$  or above will almost certainly achieve core collapse. This adds further weight to our

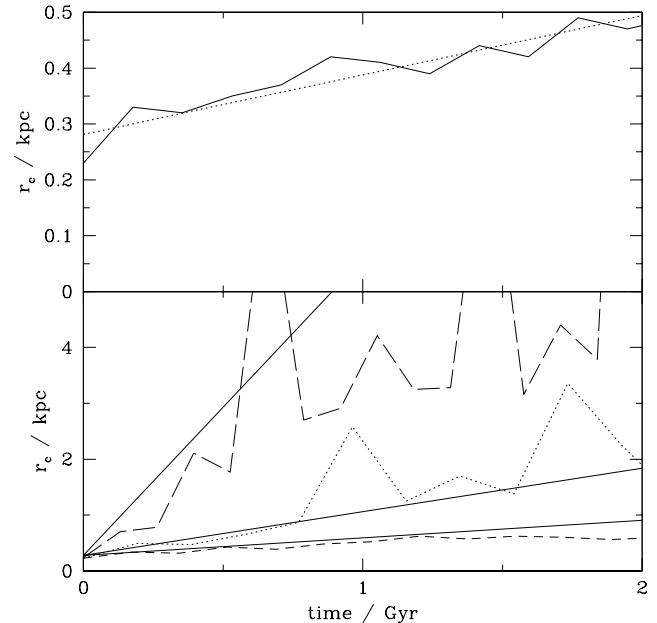


**Figure 13.** Top panel: growth of the scale radius of the tracer distribution for model 11 as a function of time (solid line). The dashed line shows the straight line fit used to describe this growth (see text for details). Bottom panel: tracer scale radius evolution for models 2 (long-dashed curve), 4 (dotted curve) and 8 (short dashed) together with predicted growth rates (solid lines) based on a rescaling of the fitted curve for model 11.

conclusion that black holes of  $10^6 M_\odot$  and above are unlikely dark matter candidates.

## 5 COMPACT INITIAL CONDITIONS

The results of the previous section demonstrate that the present stellar distribution of Draco can be preserved for a Hubble time only for black hole masses less than  $10^5 M_\odot$ . In this section we consider an alternative possibility, namely that the stellar distribution was initially significantly more compact than it is at present and was subsequently heated to its current condition by the processes described above. We now present a simple scaling argument which demonstrates that the initial conditions required are not unreasonable for black hole masses of about  $10^5 M_\odot$ .

In order to quantify the evolution of the tracer population, we fit three dimensional density profiles of the form (Zhao 1996)

$$\rho(r) = \frac{\rho_0 r_c^\gamma}{r^\alpha (r^\beta + r_c^\beta)^{(\gamma-\alpha)/\beta}}. \quad (17)$$

These profiles incorporate the Plummer profile ( $\alpha = 0$ ,  $\beta = 2$ ,  $\gamma = 5$ ) but they also include outer profiles which fall off either faster or slower than  $r^{-5}$ . The curves in Fig. 13 show the evolution of the tracer scale radii  $r_c$  obtained from fits of this form to four of our models.

The top panel of Fig. 13 shows the evolution of the scale radius of the tracer distribution in model 11 during the first 2 Gyr. Until this time, more than 70 percent of the tracers lie within one scale radius  $r_s$  of the halo. This is important,

as we expect the simple scaling arguments given below to hold only during the time when the tracers are confined to the central regions of the halo, where the density profile is a single power-law. The solid line in Fig. 13 shows the straight line fit to the temporal increase of  $r_c$

$$r_c(t) = 0.28 \left( 1 + 9.467 \left( \frac{t}{t_{\text{rh}}} \right) \right), \quad (18)$$

where  $r_c$  is in kpc. In the regime where the majority of tracers lie in the volume where the halo potential goes as  $1/r$ , the parameters of the fit should be independent of the mass of the black holes and the evolution of the scale radius can therefore be estimated from the above equation using the appropriate value for  $t_{\text{rh}}$ . For the other models, this approximation is valid for less than 2 Gyr as the tracer distribution rapidly expands into the outer regions of the halo. However, as the bottom panel of Fig. 13 demonstrates, this simple scaling argument yields a reasonable estimate of the initial growth rate of the tracer scale radius. At later times, the heating rate falls below the estimated value as the tracers no longer lie solely in the single power-law region of the halo.

We can extrapolate the scale radius evolution estimated from equation (18) to consider the evolution of tracer populations whose initial distribution is more compact than those considered so far. This extrapolation backwards in time is valid unless the initial  $r_c$  is so small that the stellar population would become self-gravitating. For example, for model 2, if we require that after 10 Gyr we have  $r_c = 232$  pc, then this implies an initial radius of 1 pc for the stellar population, which corresponds to a dense and self-gravitating stellar cluster. However, for model 11 the required initial radius is 48 pc. If this population resided in the centre of the halo, then the halo mass within its volume would be comparable to the stellar mass which would not, therefore, be self-gravitating. This suggests that the heating of the stellar population by a halo of  $10^5 M_\odot$  black holes need not be catastrophic for a dSph such as Draco, provided that its initial stellar population is sufficiently compact. It is less clear whether the same holds for black hole masses of  $10^6 M_\odot$ . In this case, the initial cluster has scale radius 8 pc and since it would therefore be almost self-gravitating, the simple scaling argument presented here breaks down.

It is important to emphasise at this point that the heating rate depends on the relative velocities of the black holes and tracers. A more compact, but not self-gravitating, initial tracer density distribution has a lower velocity dispersion and hence the rate at which it is heated is initially greater than we have estimated here. However, this increases the initial heating rate by at most a factor of two for the range of initial conditions we consider and so will not substantially affect our conclusions. There are additional heating effects to be considered for an initially small system, such as relaxation due to  $\sqrt{N}$  fluctuations in the number of black holes within the stellar distribution. These would make early expansion proceed more rapidly than otherwise. While it might be possible to balance this effect to some extent by the stabilising effects of self-gravity, we still conclude that constructing a dynamical history for Draco which results in a present-day stellar distribution with a half-light radius of 232 pc may be problematic for the scenario considered here. Further work is needed to establish the exact degree of fine tuning of the initial conditions which would be required.

If the stellar population of Draco began in a compact state and its current extent is the result of heating by black holes, it is natural to ask whether this process would lead to any clear observational signatures in either the stellar luminosity or velocity distributions. Spitzer (1987) has shown that weak encounters in  $N$ -body systems produce a population of weakly bound objects with a power-law density distribution. The logarithmic slope of this density profile depends on the gravitational potential, which is assumed also to be a single power-law. LO85 showed that strong encounters generate a profile with a different logarithmic slope to that generated by weak encounters. In our simulations, however, both weak and strong encounters with the black holes contribute to the heating of the stellar distribution. As a result, there is no simple expression for the outer slope of the resultant light distribution. If the tail generated by close encounters were sufficiently populated by stars, and could therefore be identified in the light distribution of Draco, it would argue strongly that the stellar population had been heated through close encounters. On the other hand, our results demonstrate that the absence of such a tail does not preclude the black hole model. For example, in model 5 the outer profile of the stellar distribution after 10 Gyr goes approximately as  $r^{-4.6}$  which would be indistinguishable from a Plummer law, given the magnitude of the error bars on the observed luminosity at such radii (e.g. Odenkirchen et al. 2001a). We note that the change in the slope of the light distribution in the outer parts of Draco recently identified from deep imaging (Wilkinson et al. 2004) might be indicative of such a power law halo.

The velocity distribution which arises in the black hole halo scenario is also difficult to identify unambiguously from observations. One would expect to observe a significant population of stars on radial orbits in the outer regions of a heated model as a result of the heating process. Indeed, after 10 Gyr, the anisotropy of the velocity distribution in model 5 is strongly radial in the outer parts. However, the corresponding projected velocity distribution in that model does not display any features which would unambiguously point to the strong radial bias in the velocity distribution. We conclude that the simulations presented here do not predict a unique observable signature of heating by black holes. In order to address this rather unsatisfactory situation, we will investigate the evolution of initially compact dSphs in a future paper.

In our simulations we have shown that a halo which is composed of massive black holes and which initially has an NFW density profile can be transformed into a cored halo through dynamical evolution. A number of authors have considered the role of small numbers of black holes in transforming the density profiles of cusped stellar systems into cores (e.g. Henssendorf 2003) or cusped haloes into cored haloes (e.g. Merritt & Milosavljević 2002). In these papers, the black holes were a minor constituent of the mass distribution, contrary to the case we consider in which the black holes are the dark matter and constitute the bulk of the gravitating mass. We are not aware of any simulation of the evolution of a compact stellar system in the presence of an extended halo of black holes. Of more direct relevance to our results, we note that Hernandez & Gilmore (1998) concluded that black holes with masses above  $10^5 M_\odot$  could not constitute more than  $1/8$  of the total mass of dwarf disk

galaxy haloes, as in this case dynamical friction would lead to a concentration of mass at the centre of the dwarf and a consequent observable signature in the rotation curve of the dwarf. Our results cannot be compared directly with those of Hernandez & Gilmore as their calculation assumes a smooth background halo distribution with a uniform density core, while in our models no such smooth background exists. However, it is interesting that Hernandez & Gilmore came to similar conclusions about the upper limit to the mass of any putative black hole population.

We conclude this section with a discussion of potential criticisms of our black hole halo model. First, one might argue that the probability that we would observe a significant number of dSphs at a similar phase of their evolution should be very small, which would render our compact initial conditions scenario implausible. This objection can be countered if we assume that dwarf elliptical galaxies and dSphs were originally members of the same class. Dwarf ellipticals have high stellar densities compared with the low densities of the dSphs, and observations have produced evidence for the presence of black holes in these galaxies with masses of a few million solar masses in a number of these systems (e.g. M32: Verolme et al. 2002). As we have seen, heating of a compact stellar system by a black hole halo could produce a low surface brightness object similar to a dSph. On the other hand, in some cases a single black hole might become embedded in the compact cluster protecting it from further shredding and causing the stellar density to remain high, as in M32. If there is a characteristic black hole mass, then the evolutionary time scales of all the dSphs would be similar and hence it is not surprising that we observe them today in similar evolutionary states.

A second objection to the hypothesis that black holes constitute the dark matter in dSph galaxy haloes arises from observations of the Fornax dSph. Fornax, the most luminous Local Group dSph, is surrounded by a population of five old, globular clusters. The presence of these clusters in an extended distribution about the galaxy is difficult to reconcile with the presence of a large number of black holes whose masses are comparable to those of the clusters, because close encounters between the clusters and the black holes would be expected to lead to the rapid disruption of the clusters. While this is indeed perplexing, we note that if the dark matter is composed of much lower mass particles (e.g. subatomic particles), then the extended radial distribution of the Fornax clusters is equally surprising, as dynamical friction should draw the clusters into the centre of the galaxy in a fraction of the Hubble time (e.g. Tremaine et al. 1975; Oh et al. 2000). Thus the origin of the Fornax globular clusters remains an open question and, in the absence of further data, does not provide a means of distinguishing between the conventional model for the dark matter and the proposal considered here.

There are also two sets of objects in the Milky Way halo, observations of which appear to argue against black holes as major constituents of the dark matter. If black holes were ruled out for the Milky Way halo, it would make it less likely that the dark matter in dSph galaxies could be composed of black holes, since disruption of dSphs over the lifetime of the Milky Way would pollute its halo with black holes. First, deep imaging of the Milky Way globular cluster Pal 5 has revealed the presence of long tidal tails (Odenkirchen et al.

2001b, 2003) extending to distances of about 2 kpc from the cluster. Estimates of the drift rate of stars along these tails suggest that the time required for the tails to reach their observed extent is approximately 2 Gyr (Odenkirchen et al. 2003). It has been pointed out that the spatial integrity of the streams, which implies that they are kinematically cold, may place constraints on the properties of any massive substructures present in the halo of the Milky Way (e.g. Dehnen et al. 2004). In particular, simulations by Moore (priv. comm.) suggest that the tails of Pal 5 rule out a significant population of black holes with masses of about  $10^6 M_\odot$  in the halo of the Milky Way. However, we note that similar arguments apply to the substructure which is ubiquitous in standard cold dark matter simulations and thus the tails of Pal 5 do not constitute a clear observational test of the black hole model. We also note that Dehnen et al. (2004) have shown that  $N$ -body simulations of the tidal disruption of Pal 5 in a smooth Milky Way halo are unable to reproduce the observed internal structure in the stellar density distribution along the tails. Those authors suggest that the presence of an amount of halo substructure may be required to account for the non-uniform distribution of stars along the tails of Pal 5.

Recent work on the distribution of separations of wide stellar binaries in the halo of the Milky Way may constitute the strongest observational argument against the black hole halo model. In a comprehensive study of this issue, Yoo et al. (2004) show that encounters between wide binaries and massive compact objects would result in the power-law tail of binary separations becoming steeper with time. They argue that the absence of a cut-off in the distribution of wide binary separations in a large sample of nearby halo binaries rules out the presence of compact objects with masses above  $43 M_\odot$  at the standard local halo density. This analysis assumes that all the binaries in their sample have been part of the Galactic halo for at least 10 Gyr and during that time have experienced a density of dark matter comparable to the local halo density. Given that most of the halo binaries were probably formed in star clusters, it is not clear how long they have been exposed directly to potentially disrupting encounters with halo substructure. Further, if the binaries originated in halo star clusters on highly elongated orbits, they may have spent much of their lives in regions where the dark matter density is significantly lower than in the solar neighbourhood. We conclude that without information about the actual distribution of ages for the halo binaries (i.e. how long they have been part of the halo) and knowledge of the orbital distribution of the binaries in the Galactic halo, the population of wide binaries is not yet sufficient to rule out definitively massive objects as a significant component of the dark matter. However, these data have the potential to rule out black hole dark matter and therefore merit further analysis to determine their orbital properties.

## 6 SUMMARY AND CONCLUSIONS

The high mass-to-light ratios of certain Local Group dwarf galaxies suggest that they are among the most dark matter-dominated stellar systems known in the Universe. This makes them ideal laboratories in which to investigate the nature and properties of dark matter. In addition, their rel-

ative proximity has allowed the accumulation of a wealth of high quality stellar kinematic data in recent years. We present here the results of simulations where the modelled system is assumed to consist of a dwarf galaxy-sized stellar population, which initially resides in the centre of an extended, massive halo with an NFW profile. The halo particles are assigned masses of between  $10^5 M_\odot$  and  $10^7 M_\odot$  and are modelled as massive black holes. The mass of the system is chosen to match that of the Draco dSph, a Galactic satellite for which evidence has recently been presented of the existence of a massive dark matter halo (Kleyna et al. 2001). The stellar distribution appears to have suffered only minor tidal distortion (Klessen et al. 2003; Wilkinson et al. 2004). This, together with the availability of stellar velocity measurements up to four Plummer radii (Kleyna et al. 2002; Wilkinson et al. 2004), makes Draco a useful test candidate for comparison with simulations.

The first question which our simulations address is whether the black hole population evolves too quickly to be consistent with the potential observed for Draco. Perusal of the very short central relaxation times (Table 1) indicates that we might have expected the systems to undergo core collapse and re-expansion within a Hubble time, with subsequent dissolution in a Galactic tidal field, had the initial conditions been closer to a Plummer model (Lee & Ostriker 1987). However, due to the inverted initial temperature profile of the NFW model, the evolution in our simulations is slower and initially in the opposite direction, towards a lower central density with a cored rather than a cusped density profile. Only systems with black hole mass greater than  $10^{6.5} M_\odot$  appear to evolve too rapidly towards core collapse. For the lower end of the mass range investigated, evolution leads to a profile with a density profile that is more consistent with observations of dSphs (Kleyna et al. 2003; Magorrian 2003) than the initial NFW model.

A more serious set of issues is raised by the evolution of the tracer populations. We find that in all of our dSph-sized models, the central tracer density shows a very rapid decline in the first Gyr, corresponding to over-efficient heating by the black holes. This effect can also be observed via the increase in the tracer velocity dispersion, which at 10 Gyr cannot be reconciled with the observed Draco dispersion. If the initial stellar distribution is chosen to match that of Draco, then only for black holes of mass below about  $10^5 M_\odot$  is the heating rate reduced to a level which could perhaps be compatible with the observations. We conclude that the haloes of dSph galaxies cannot be composed of black holes more massive than  $10^5 M_\odot$  if their initial stellar distributions were similar to those observed at the present time.

We have also performed simulations in which the scale length was set to twice that used to model the halo of Draco. The heating of the stellar population in these cases was somewhat reduced, and more than 10 percent of the stellar population which initially occupied the central 500 pc of the halo remained in this region after 10 Gyr for black hole masses of  $10^6 M_\odot$ , as opposed to a loss of greater than 95 percent for the models with smaller  $r_s$ . However, the velocity dispersion of the evolved tracers within the same region is still uncomfortably large. Notwithstanding the question of how to suppress the heating of the stellar population, the evolution of the haloes of these models is potentially very interesting. As Fig. 3 shows, the inner regions of the haloes

evolve towards a more cored profile. Thus, these models may be able to explain the observations of LSB galaxies which appear to have large dark matter cores (de Blok & Bosma 2002).

By constraining the amount of evolution allowed to take place for the stellar population within a given time scale, we are able to place a new upper limit on the mass of individual black holes which constitute the dark matter halo of Draco. If we require that the stellar count within 500 pc of the halo origin decreases by no more than a factor of 2 within 5 Gyr, we obtain an upper mass constraint of approximately  $10^5 M_\odot$ ; the equivalent condition required over a time scale of 10 Gyr sets a limit of  $10^{4.6} M_\odot$ . These numbers call into question the hypothesis that massive black holes could be a significant component of the dark matter: black holes with masses below  $10^5 M_\odot$  are less interesting as dark matter candidates because they cannot explain either the heating of the Milky Way disk (LO85) or the origin of cores in dark haloes (Section 4.4). Therefore, we have also investigated the possibility that a dSph whose initial stellar distribution was more compact than those of the present-day dSphs could evolve into an object resembling Draco as a result of heating. We have presented a simple scaling argument which implies that if the black holes have masses of  $10^5 M_\odot$  then an initial stellar distribution with scale radius 48 pc would evolve into an object of similar extent to that of Draco in 10 Gyr; such a scenario may permit models with black hole masses somewhat larger than  $10^5 M_\odot$  and correspondingly more compact initial conditions. However, we note that this scenario may require very finely tuned initial conditions because  $\sqrt{N}$  noise in the black hole distribution may inflate the heating rate at early times.

In summary, we find that scenarios in which the dark matter is in the form of massive black holes, with masses between  $10^5 M_\odot$  and a few  $\times 10^5 M_\odot$ , may provide a viable channel for the production of cored, rather than cusped, haloes but only if the initial stellar distributions of the dSphs were considerably more compact than the currently observed ones. Further simulations will be required to determine if this picture is, in all details, consistent with the observed data on the Local Group dSphs.

## Acknowledgements

We thank Scott Tremaine for valuable comments on an earlier draft of this paper and Sverre Aarseth for many useful discussions and for the use of his NBODY codes. We thank Andy Gould, Bohdan Paczynski, Piotr Popowski, Paolo Salucci and F. Javier Sanchez for their critical comments on the feasibility of the models, and the anonymous referee for useful comments. MIW acknowledges financial support from PPARC.

## REFERENCES

- Aarseth S. J., 1999, *Celestial Mechanics and Dynamical Astronomy*, 73, 127
- Aarseth S. J., 2001, *New Astronomy*, 6, 277
- Binney J., Tremaine S., 1987, *Galactic dynamics*. Princeton, NJ, Princeton University Press
- Binney J. J., Evans N. W., 2001, *MNRAS*, 327, L27

- Borriello A., Salucci P., Danese L., 2003, MNRAS, 341, 1109
- Bullock J. S., Kolatt T. S., Sigad Y., Somerville R. S., Kravtsov A. V., Klypin A. A., Primack J. R., Dekel A., 2001, MNRAS, 321, 559
- Cohn H., 1980, ApJ, 242, 765
- Colin P., Klypin A., Valenzuela O., Gottlober S., 2003, astro-ph/0308348
- de Blok W. J. G., Bosma A., 2002, A&A, 385, 816
- De Lucia G., Kauffmann G., Springel V., White S. D. M., Lanzoni B., Stoehr F., Tormen G., Yoshida N., 2004, MNRAS, 348, 333
- Dehnen W., 2003, MNRAS, 265, 250
- Dehnen W., Odenkirchen M., Grebel E. K., Rix H., 2004, AJ, 127, 2753
- Fukushige T., Makino J., 2001, ApJ, 557, 533
- Ghigna S., Moore B., Governato F., Lake G., Quinn T., Stadel J., 2000, ApJ, 544, 616
- Giersz M., Heggie D. C., 1996, MNRAS, 279, 1037
- Giersz M., Heggie D. C., 1997, MNRAS, 286, 709
- Gnedin O. Y., Ostriker J. P., 2001, ApJ, 561, 61
- Hayashi E., Navarro J. F., Taylor J. E., Stadel J., Quinn T., 2003, ApJ, 584, 541
- Heggie D. C., Mathieu R. D., 1986, in LNP Vol. 267: The Use of Supercomputers in Stellar Dynamics p. 233
- Helmi A., White S. D. M., 2001, MNRAS, 323, 529
- Hensendorff M., 2003, Ap&SS, 284, 561
- Hernandez X., Gilmore G., 1998, MNRAS, 297, 517
- Irwin M., Hatzidimitriou D., 1995, MNRAS, 277, 1354
- Kazantzidis S., Magorrian J., Moore B., 2004, ApJ, 601, 37
- Keeton C. R., 2003, ApJ, 584, 664
- Klessen R. S., Grebel E. K., Harbeck D., 2003, ApJ, 589, 798
- Klessen R. S., Kroupa P., 1998, ApJ, 498, 143
- Kleyna J., Wilkinson M. I., Evans N. W., Gilmore G., Frayn C., 2002, MNRAS, 330, 792
- Kleyna J. T., Wilkinson M. I., Evans N. W., Gilmore G., 2001, ApJ, 563, L115
- Kleyna J. T., Wilkinson M. I., Gilmore G., Evans N. W., 2003, ApJ, 588, L21
- Lacey C. G., Ostriker J. P., 1985, ApJ, 299, 633
- Lee H. M., Ostriker J. P., 1987, ApJ, 322, 123
- Li L., Ostriker J. P., 2002, ApJ, 566, 652
- Magorrian J., 2003, in The Mass of Galaxies at Low and High Redshift. Proceedings of the ESO Workshop held in Venice, Italy, 24-26 October 2001 p. 18
- Makino J., Taiji M., Ebisuzaki T., Sugimoto D., 1997, ApJ, 480, 432
- Mao S., Jing Y., Ostriker J. P., Weller J., 2004, ApJ, 604, L5
- Mateo M. L., 1998, ARA&A, 36, 435
- Merritt D., Milosavljević M., 2002, in Dark matter in astrophysics and particle physics. Proceedings of the International Conference DARK 2002, H. V. Klapdor-Kleingrothaus, R. D. Viollier (eds.). Physics and astronomy online library. Berlin: Springer, 2002 p. 79
- Metcalf R. B., Madau P., 2001, ApJ, 563, 9
- Mikkola S., Aarseth S. J., 1993, Celestial Mechanics and Dynamical Astronomy, 57, 439
- Mikkola S., Aarseth S. J., 1998, New Astronomy, 3, 309
- Moore B., Ghigna S., Governato F., Lake G., Quinn T., Stadel J., Tozzi P., 1999, ApJ, 524, L19
- Navarro J. F., Frenk C. S., White S. D. M., 1996, ApJ, 462, 563
- Navarro J. F., Frenk C. S., White S. D. M., 1997, ApJ, 490, 493
- Odenkirchen M., Grebel E. K., Dehnen W., Rix H., Yanny B., Newberg H. J., Rockosi C. M., Martínez-Delgado D., Brinkmann J., Pier J. R., 2003, AJ, 126, 2385
- Odenkirchen M., Grebel E. K., Harbeck D., Dehnen W., Rix H., Newberg H. J., Yanny B., Holtzman J., et al. 2001a, AJ
- Odenkirchen M., Grebel E. K., Rockosi C. M., Dehnen W., Ibata R., Rix H., Stolte A., Wolf C., et al. 2001b, ApJ
- Oh K. S., Lin D. N. C., Richer H. B., 2000, ApJ, 531, 727
- Ostriker J. P., Gnedin N. Y., 1996, ApJ, 472, L63
- Ostriker J. P., Steinhardt P., 2003, Science, 300, 1909
- Plummer H. C., 1911, MNRAS, 71, 460
- Ricotti M., 2003, MNRAS, 344, 1237
- Salucci P., 2001, MNRAS, 320, L1
- Spergel D. N., Steinhardt P. J., 2000, Physical Review Letters, 84, 3760
- Spitzer L., 1987, Dynamical evolution of globular clusters. Princeton, NJ, Princeton University Press
- Stoehr F., White S. D. M., Tormen G., Springel V., 2002, MNRAS, 335, L84
- Suto Y., 2002, in S. B., Hwang C.-Y., eds, in "Matter and Energy in Clusters of Galaxies"
- Swaters R. A., Madore B. F., van den Bosch F. C., Balcells M., 2003, ApJ, 583, 732
- Tremaine S. D., Ostriker J. P., Spitzer L., 1975, ApJ, 196, 407
- Verolme E. K., Cappellari M., Copin Y., van der Marel R. P., Bacon R., Bureau M., Davies R. L., Miller B. M., de Zeeuw P. T., 2002, MNRAS, 335, 517
- Wilkinson M. I., Kleyna J., Evans N. W., Gilmore G., 2002, MNRAS, 330, 778
- Wilkinson M. I., Kleyna J. T., Evans N. W., Gilmore G. F., Irwin M. J., Grebel E. K., 2004, ApJ, 611, L21
- Yoo J., Chanamé J., Gould A., 2004, ApJ, 601, 311
- Zhao H., 1996, MNRAS, 278, 488